Online Supplemental Material

Supplemental Figure Legends

Figure S1. KLP59D immunostaining in mitotic S2 cells. A) Immunofluorescence images showing the localization of KLP59D throughout mitosis in S2 cells (except anaphase which is shown in figure 1A). **B)** Image of a live S2 cell expressing eGFP-KLP10A and mRFP-α-tubulin. **C)** Metaphase S2 cells double-labeled for KLP10A and α-tubulin. KLP10A localizes to the spindle poles as well as the centrosomes and kinetochores during mitosis. Yellow arrows indicate spindle pole localization of KLP10A.

Figure S2. KLP59D regulates α-Tubulin turnover at metaphase. A) Representative fluorescence recovery plots measured from eGFP-α-tubulin labeled metaphase spindles photobleached at spindle poles (containing primarily minus-ends) and equators (containing primarily plus-ends). **B)** Average percentages of total original fluorescence recovered after photobleaching. Numbers in bars are N.

Figure S3. KLP59D targets KLP10A to the centrosomes independently of microtubules. **A)** Representative examples of colchicines treated RNAi-treated cells fixed, immunostained with anti-KLP10A (red) and anti-γ-tubulin (green), and imaged using identical methods. Right panel shows only KLP10A labeling. **B)** Average KLP10A immunofluorescence intensities at centrosomes. Values are normalized so that control RNAi intensities are 100%. KLP10A levels decrease ~40% upon KLP59D RNAi. *

indicates statistical significance (P<0.0001). N indicated in each bar and error bars=SEM.

Figure S4. Depletion of KLP59D disrupts the pole localization of Asp. A) Immunofluorescence images showing Asp localization in control and KLP59D RNAi treated spindles acquired with identical conditions and presented as in Figure 6. **B)** Graph showing the comparison of the levels of pole associated Asp in control and KLP59D RNAi treated cells. N indicated in each bar. Asterisk indicates statistical significance (p<0.01). **C)** Transgenic KLP59D-eGFP co-precipitates endogenous KLP10A from mitotic (M) cell lysate, and vice versa. Western blots were probed with the indicated antibodies. "KLP59D-GFP M-Lysate", Lysate of mitotic S2 cells expressing GFP tagged KLP59D; "Beads", protein-G beads only; "ip", immunoprecipitate. **D)** Western blots of immunoprecipitations from mitotic cell extracts transfected with the indicated constructs tagged with GFP. KLP59D-eGFP and KLP10A-eGFP each co-immunoprecipitates with its endogenous wild-type isoform. "M-Lysate", Lysate of mitotic S2 cells expressing GFP tagged KLP59D/KLP10A; "Beads", protein-G beads only; "ip", immunoprecipitate.

Figure S5. KLP59D disassembles microtubules *in vitro*. Purified, full-length His-tagged KLP59D at the indicated concentrations was incubated with taxol-stabilized microtubules (1μM) and Mg-ATP, and the turbidity (at 350nm) measured as a function of time. Increasing KLP59D concentration increases the rate of turbidity reduction.

Figure S6. Depletion of KLP59C, but not KLP59D, increases the percentage of anaphase cells with lagging chromosomes. Averages for the KLP59C RNAi and 59D/59C co-RNAi treatments are not significantly different, but are significantly different than both the control and KLP59D RNAi treatments (double asterisks).

Supplemental Movies

Movie S1. A control RNAi S2 cell in anaphase A. The spindle microtubules can be visualized because of the constitutive expression of eGFP-α-tubulin. The poleward movement of chromatids attached to the fluorescent kMTs can be inferred from the shortening lengths of kMTs.

Movie S2. Anaphase A in a KLP59D RNAi S2 cell expressing eGFP-α-tubulin. The kMTs shorten at a noticeably slower rate than seen in controls (Movie 1). Therefore, the chromatid-to-pole velocity is reduced by depletion of KLP59D.

Movie S3. Flux and Pacman rates can be measured in live S2 cells expressing eGFP-α-tubulin and whose chromosomes are Hoechst stained. This S2 cell has been treated with control RNAi. Lines are photobleached across the fluorescent microtubules of each half spindle. Pacman is measured as the rate that chromosomes move relative to the bleached lines. Poleward flux is measured as the rate that the bleached lines move to the spindle poles.

Movie S4. Flux and Pacman in a KLP59D RNAi treated cell. Both types of motility are decreased compared to their control counterparts (Movie S3).

Supplementary Figure S1

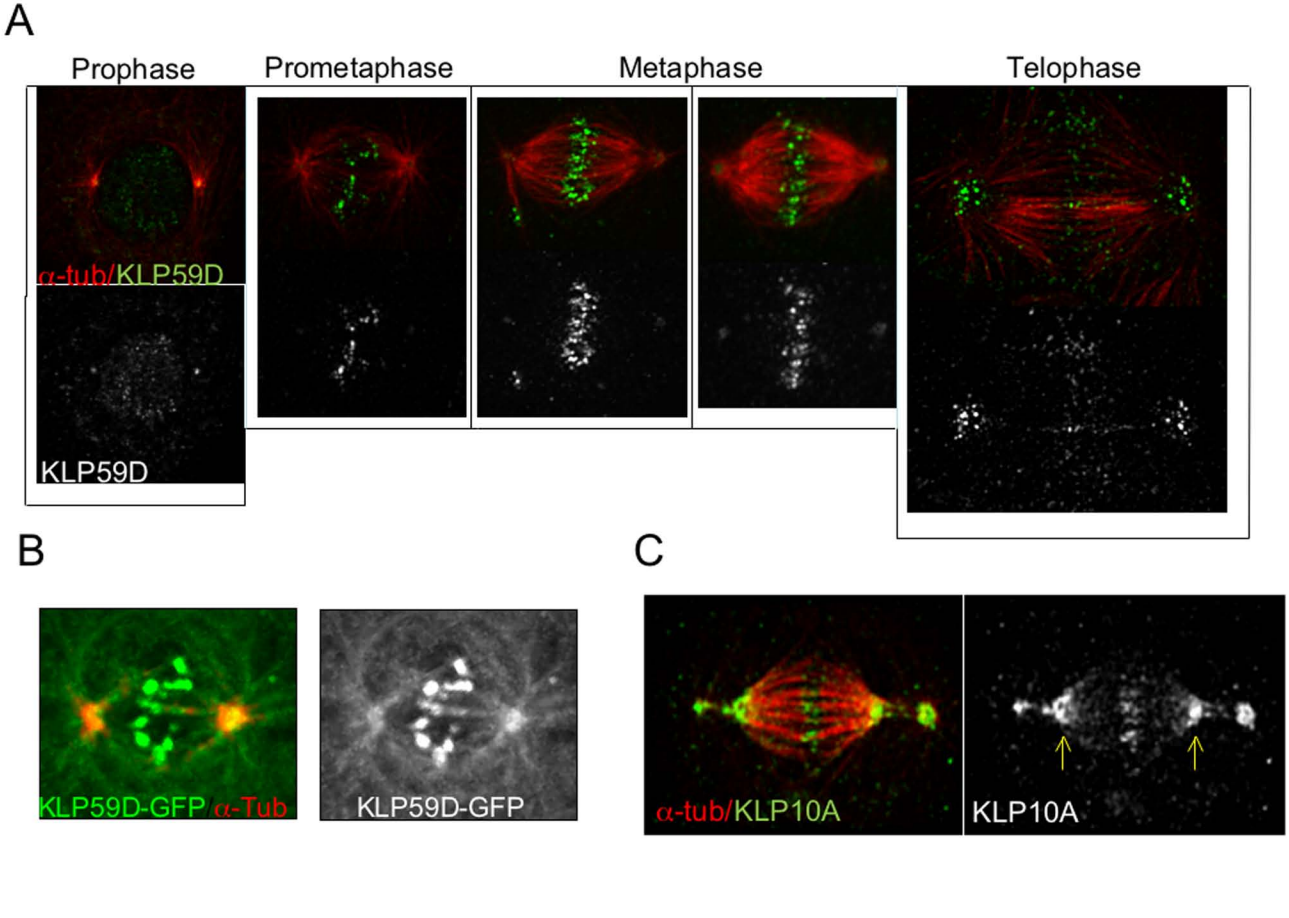

A

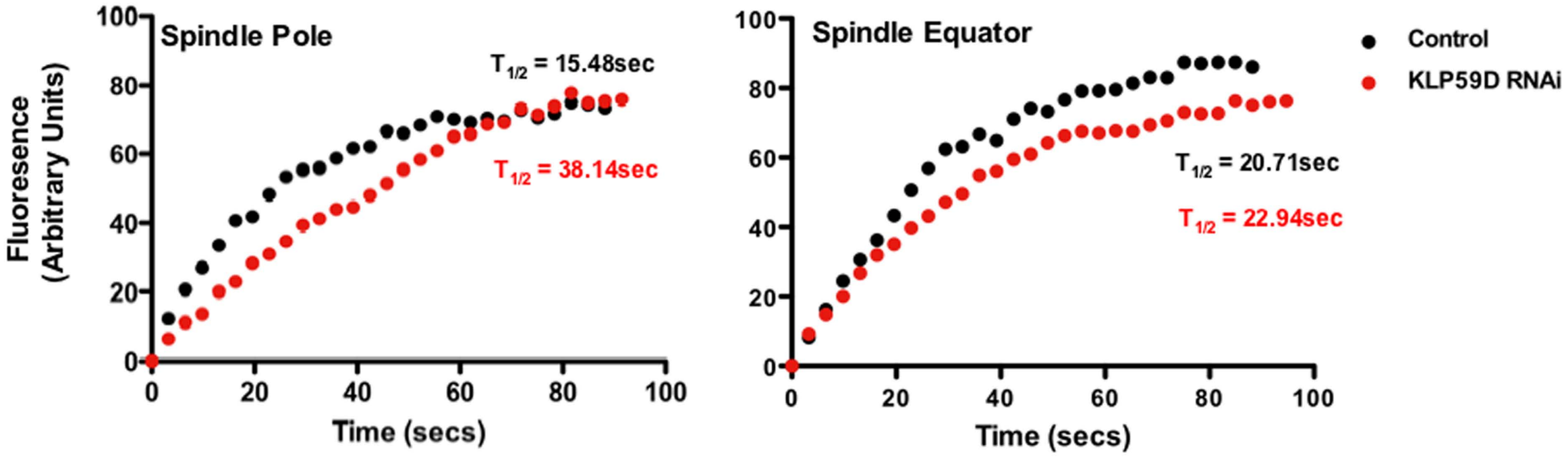
Spindle Pole
$T_{1/2}$ = 15.48sec
$T_{1/2}$ = 38.14sec
Fluoresence (Arbitrary Units)
Time (secs)
Spindle Equator
$T_{1/2}$ = 20.71sec
$T_{1/2}$ = 22.94sec
Time (secs)
Control
KLP59D RNAi

B

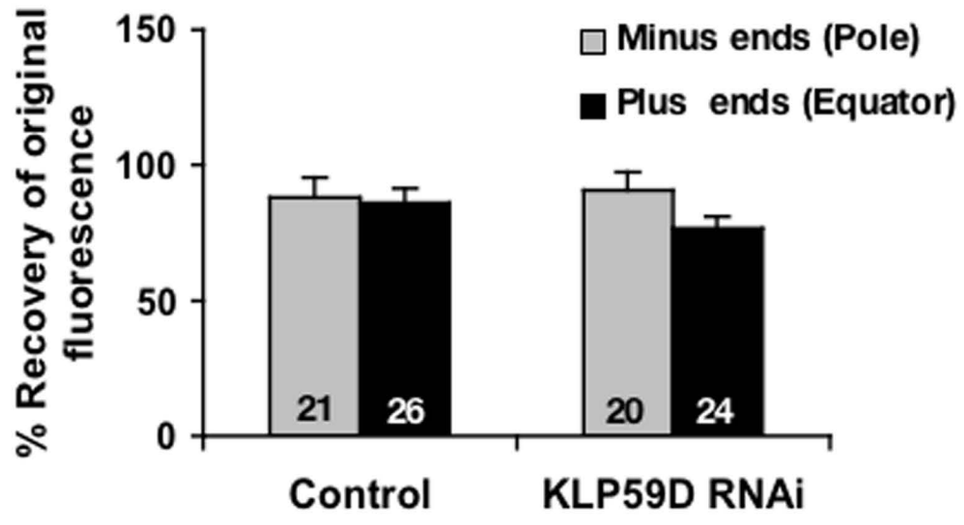
% Recovery of original fluorescence
Minus ends (Pole)
Plus ends (Equator)
21
26
20
24
Control
KLP59D RNAi

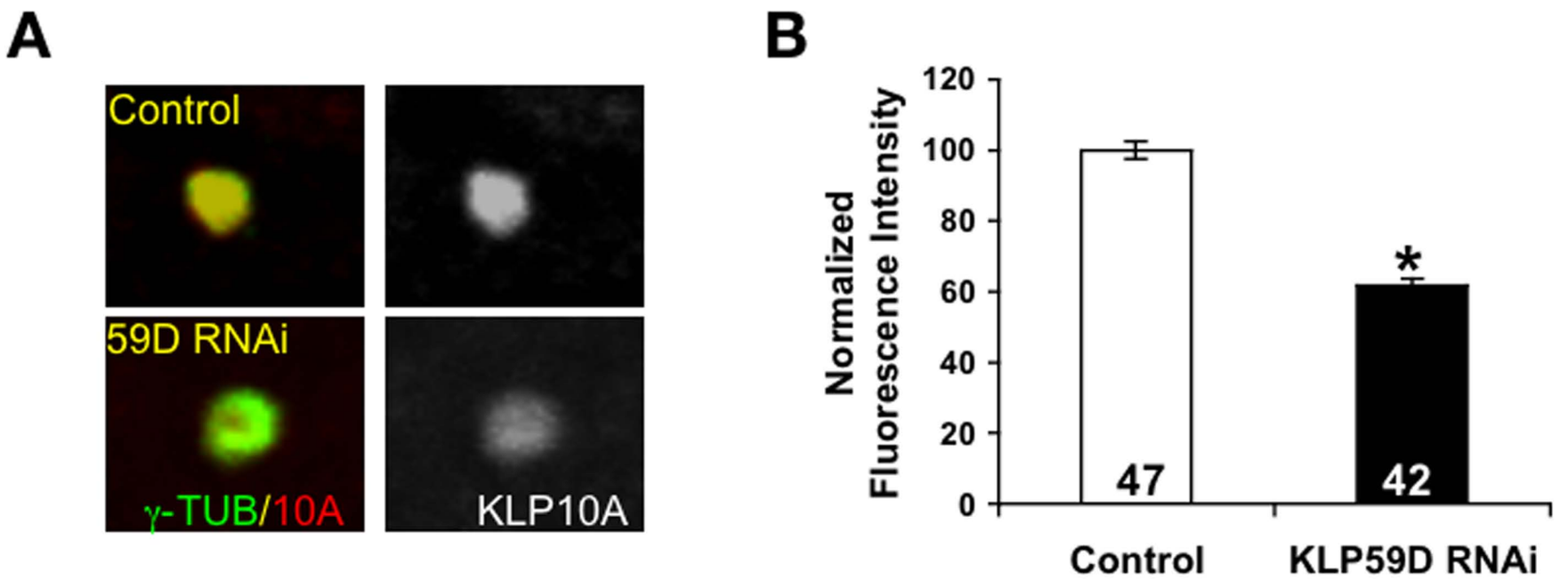
A
Control
59D RNAi
γ-TUB/10A
KLP10A
B
Normalized Fluorescence Intensity
120
100
80
60
40
20
0
47
42
*
Control
KLP59D RNAi

Supplemental Figure S4

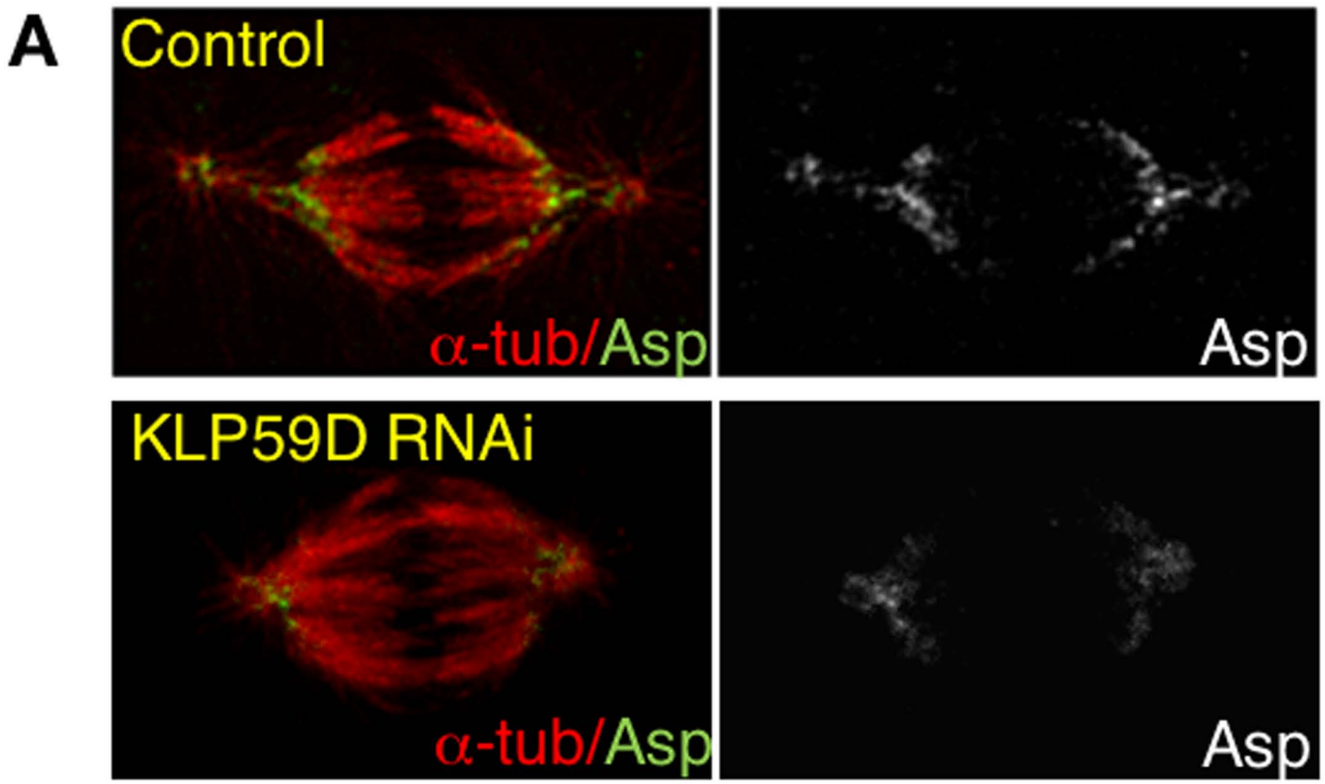

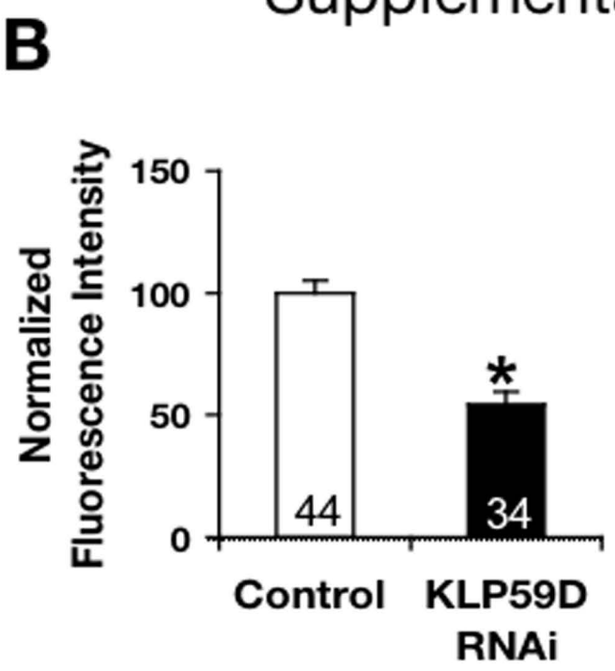

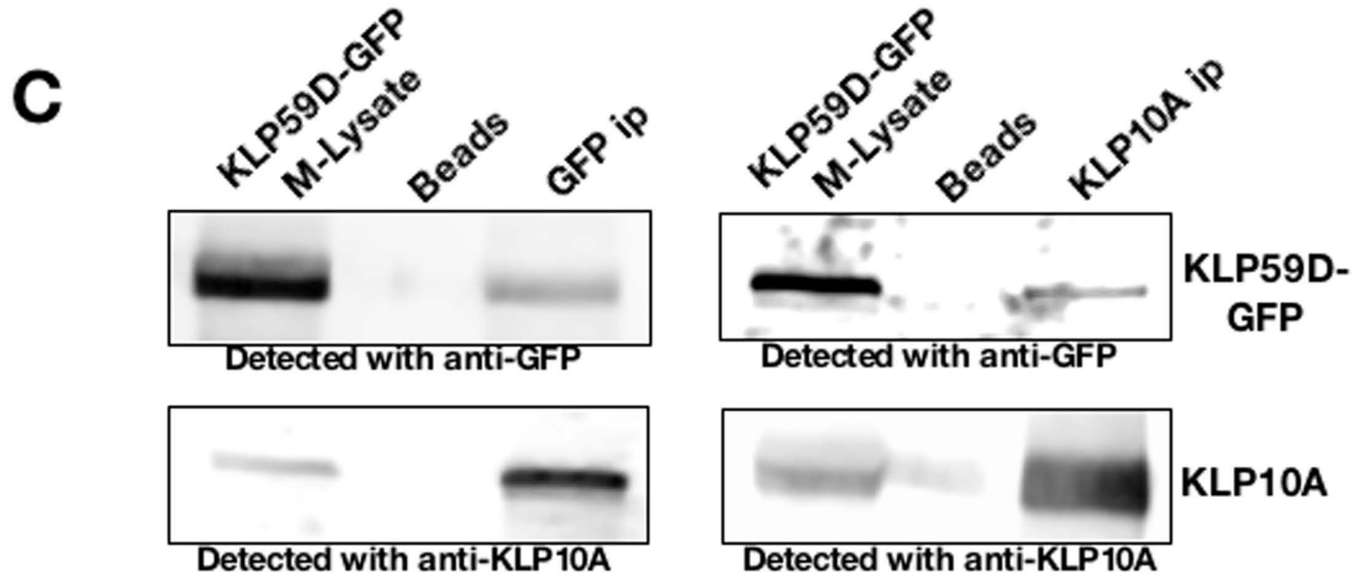

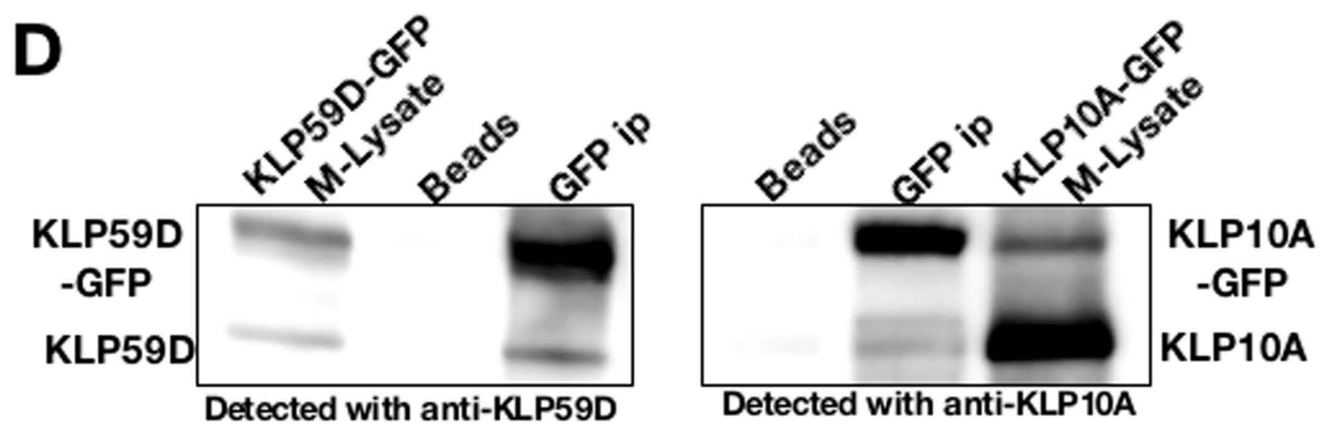

Supplemental Figure S5

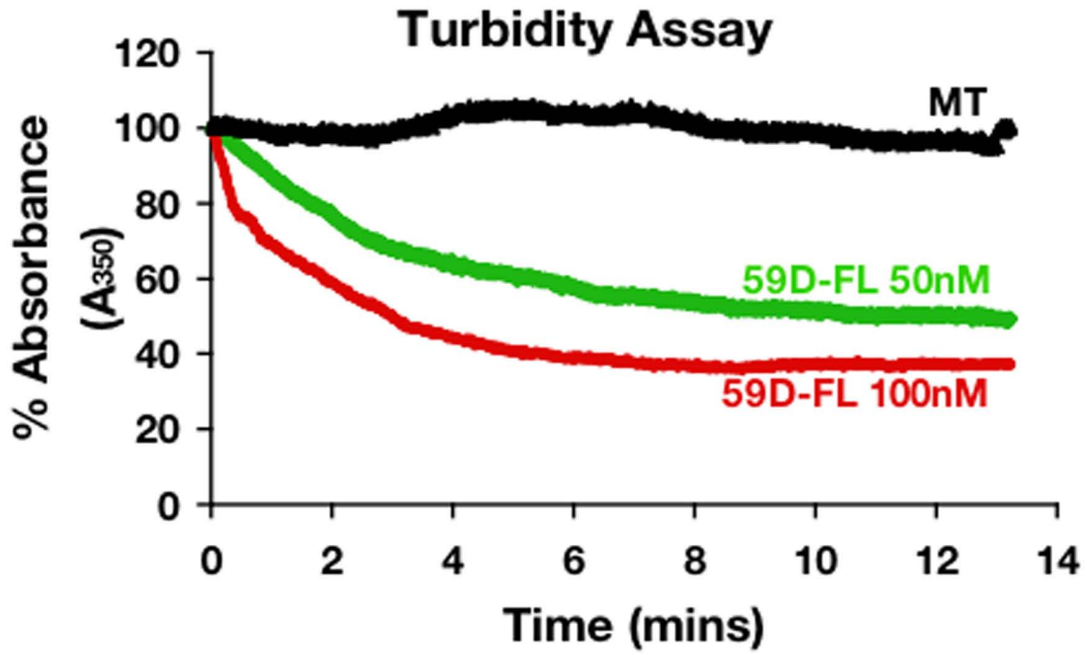

Supplemental Figure S6

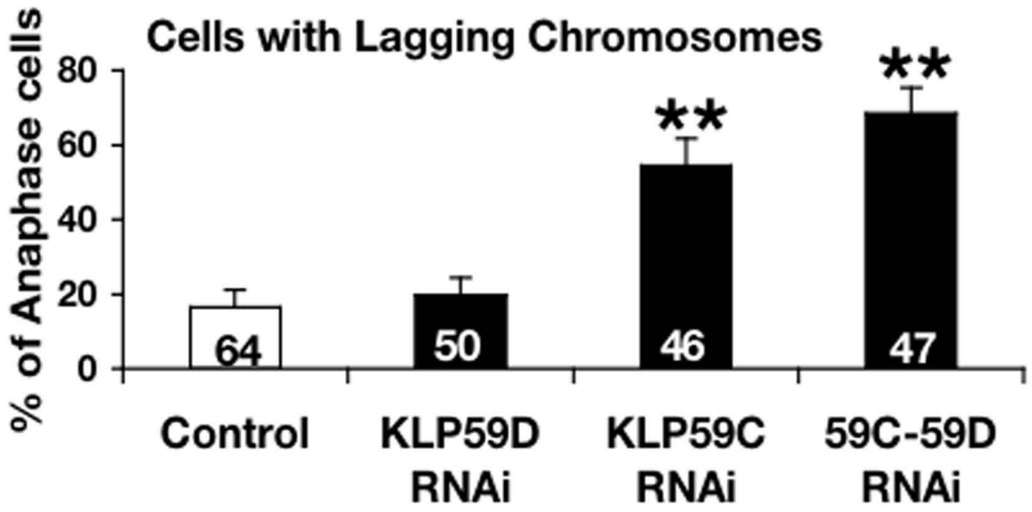

Supplemental Table S1

RNAi Treatments	Metaphase FLUX (μm/min) (N, p value)	Anaphase FLUX (μm/min) (N, p value)	Anaphase PACMAN (μm/min) (N, p value)	Anaphase A CHROMATID-TO-POLE (μm/min) (N, p value)
CONTROL	1.09±0.08 (N=99)	0.93±0.05 (N=68)	0.81±0.05 (N=68)	1.4±0.05 (N=68)
KLP59D RNAi	0.4±0.07 (N=61, p<0.001)	0.50±0.04 (N=45, p<0.001)	0.18±0.05 (N=45, p<0.001)	0.7±0.06 (N=45, p<0.001)
KLP10A RNAi	0.34±0.04 (N=48, p<0.001)	0.28±0.04 (N=37, p<0.001)	0.50±0.06 (N=37, p<0.001)	0.8±0.07 (N=37, p<0.001)
KLP59C RNAi	1.06±0.07 (N=30, p=0.75)	0.93±0.05 (N=56, p=0.77)	0.73±0.04 (N=56, p=0.13)	1.2±0.06 (N=56, p=0.22)

Phenotypes	Control RNAi (%, N)	KLP59D RNAi (%, N, p value)
Monopolar spindles	10.12±0.09 (1930)	25±0.12 (1596, p=0.02)
Multinucleate cells	5.96±0.02 (1056)	10.65±0.02 (1051, p<0.001)